Journal of *Marine Science and Engineering*

MDPI

Article

Research on Bearing Fault Diagnosis Method of the FPSO Soft Yoke Mooring System Based on Minimum Entropy Deconvolution

Yanlin Wang [1], Jiaxi Zhang [1], Shanshan Sun [2], Zheliang Fan [1], Dayong Zhang [1], Ziguang Jia [1,*], Peng Zhang [3,*] and Yi Huang [4]

[1] School of Chemical Engineering, Ocean and Life Sciences, Dalian University of Technology, Panjin 124221, China; wangyl@dlut.edu.cn (Y.W.); zhangjx1@mail.dlut.edu.cn (J.Z.); fanzl@dlut.edu.cn (Z.F.); zhangdy@dlut.edu.cn (D.Z.)
[2] School of General Education, Dalian University of Technology, Panjin 124221, China; sunss@dlut.edu.cn
[3] College of Transportation Engineering, Dalian Maritime University, Dalian 116026, China
[4] School of Naval Architecture & Ocean Engineering, Dalian University of Technology, Dalian 116024, China; huangyi@dlut.edu.cn
* Correspondence: jiaziguang@dlut.edu.cn (Z.J.); peng.zhang47@dlmu.edu.cn (P.Z.)

Abstract

The Soft Yoke Mooring (SYM) system is a critical single-point mooring method for Floating Production Storage and Offloading systems (FPSOs) in shallow waters. Its articulated thrust roller bearing operates long-term in harsh marine environments, making it prone to failure and difficult to diagnose. To address the issues of non-stationary signals and fault features submerged in strong noise caused by the bearing's non-rotational oscillatory motion, this paper proposes an adaptive improved diagnosis scheme based on Minimum Entropy Deconvolution (MED). By optimizing Finite Impulse Response (FIR) filter parameters to adapt to the oscillatory operating conditions and combining joint analysis of time-domain indicators and envelope spectra, precise identification of bearing faults is achieved. Research shows that this method effectively enhances fault impact components. After MED processing, the kurtosis value of the fault signal can be significantly increased from approximately 2.6 to over 8.6. Its effectiveness in noisy environments was verified through simulation. Experiments conducted on a 1:10 scale soft yoke model demonstrated that the MED denoising and filtering signal analysis method can effectively identify damage in the thrust roller bearing of the SYM system under marine conditions characterized by high noise and complex frequencies. This study provides an efficient and reliable method for fault diagnosis of non-rotational oscillatory bearings in complex marine environments, holding significant engineering application value.

Keywords: soft yoke mooring system; minimum entropy deconvolution; thrust roller bearing; fault diagnosis; signal analysis

Check for updates

Academic Editor: Erkan Oterkus

Received: 30 December 2025
Revised: 19 January 2026
Accepted: 21 January 2026
Published: 22 January 2026

Copyright: © 2026 by the authors. Licensee MDPI, Basel, Switzerland. This article is an open access article distributed under the terms and conditions of the Creative Commons Attribution (CC BY) license.

1. Introduction

Floating Production Storage and Offloading system (FPSO), with its exceptional reliability, adaptability to the marine environment, and cost-effectiveness, has become the mainstream equipment for offshore oil development in the Bohai Sea of China. The Soft Yoke Mooring (SYM) system is one of the more commonly used mooring methods. Currently, research on fault diagnosis for bearings in SYM systems is scarce. Existing studies primarily focus on field monitoring of the overall structural safety and motion characteristics of mooring systems, analyzing the safety issues of SYM systems under extreme

sea conditions and providing early warnings [1–3]. However, research on monitoring and diagnosis specifically targeting the thrust roller bearing at the articulated joint of the mooring leg is relatively limited, mainly employing methods combining displacement monitoring, strain monitoring, video surveillance, and disassembly inspection [4].

In the broader field of mechanical diagnosis, bearing condition monitoring often relies on multi-parameter analysis such as temperature, vibration, and clearance [5]. For instance, in industrial robot systems, monitoring changes in bearing temperature, vibration velocity, and axial/radial clearances has been proven effective for collaboratively assessing their operational status and reliability [6]. Concurrently, diagnostic methods based on thermal analysis, such as establishing a quantitative relationship between bearing surface temperature and internal frictional temperature through finite element simulation, provide a theoretical foundation for automatic bearing condition monitoring [7]. However, the direct application of these methods faces challenges in the specific context of marine engineering.

The marine environment is filled with strong noise and issues like salt spray corrosion and humidity [8]. Sensors for multi-parameter monitoring methods (vibration, temperature) suffer from extremely low signal-to-noise ratios in such conditions, making the collected signals easily submerged and fault features difficult to extract. Furthermore, the thrust roller bearing at the FPSO soft yoke articulated joint is typically encapsulated within the mooring leg structure, in a semi-enclosed or fully enclosed state. This not only makes optimal placement of vibration and temperature sensors extremely difficult but also significantly reduces the effectiveness of thermal imaging or external temperature measurement, as the heat transfer path is complex, and the temperature measured on the surface cannot accurately reflect the true state of the internal bearing friction points.

Meanwhile, in the general technical field of bearing fault diagnosis, vibration signal analysis is the most widely used core method, giving rise to various time-frequency domain analysis techniques. Among them, time-frequency signal analysis methods like Short-Time Fourier Transform (STFT) and wavelet analysis have been applied to the fault diagnosis of conventional mechanical bearings, but they have significant limitations: STFT has fixed time-frequency resolution, making it difficult to adapt to the dynamic characteristics of non-stationary signals in the marine environment; the effectiveness of wavelet analysis highly depends on the selection of the wavelet basis function, and the feature extraction results for the same fault signal can vary greatly with different basis functions. Under strong noise interference, the feature recognition capabilities of both methods are significantly weakened [9].

Additionally, cost-effectiveness is an important consideration for bearing maintenance and repair strategies. Research in the agricultural machinery field indicates that for vulnerable universal joint bearing assemblies, a repair method involving rotating the unworn surface to the load-bearing area and replacing the needle roller bearing can significantly reduce costs compared to overall repair or replacement with new components, offering ideas for the sustainable maintenance of high-value equipment bearings [10]. However, none of these methods are optimized for the distinctive ‘non-rotational oscillatory’ operating condition of the FPSO soft yoke bearing.

Minimum Entropy Deconvolution, as a blind deconvolution method, has its core advantage in enhancing deterministic impact components by minimizing the amplitude spectrum entropy of the signal, without relying on prior signal or transfer path information. It has shown unique value in extracting weak fault features of rolling element bearings. Initially proposed by Wiggins for seismic signal processing, it has later been widely applied to the fault diagnosis of rotating machinery bearings [11]. It can effectively separate fault impact signals masked by noise and harmonics, significantly improving the identifiability of fault features [12]. However, unlike traditional rotating bearings, the thrust roller bearing

in the FPSO mooring leg undergoes pendulum-like motion following the vessel's pitch, characterized by a non-linear trajectory, non-fixed rotational speed, and undefined fault characteristic frequencies. Existing MED application schemes based on the assumption of pure rotational motion cannot be directly adapted [13].

In SYM systems, the bearings at the upper and lower articulated joints of the mooring leg serve as the pivotal hubs for its multi-rigid-body motion. Diagnosing faults in these bearings is crucial. Once they fail, the local degrees of freedom of the soft yoke become locked, disrupting the coordinated motion of the entire system. In mild cases, this leads to abnormal friction, severe noise, and component wear, accelerating structural fatigue. In severe cases, obstructed motion causes load redistribution, generating unforeseen stress concentrations within the mooring leg structure. This may trigger a chain of failures, such as joint fracture or ballast tank tilting. Such failures not only threaten the safety of the single-point platform and the FPSO itself but may also lead to catastrophic consequences including mooring failure and production shutdown [14]. Therefore, monitoring and diagnosing the condition of these bearings—such as wear and seizure—is paramount for preventing kinematic domain failure of the soft yoke and ensuring the safe operation of the entire shallow-water mooring system.

This paper proposes an innovative fault diagnosis scheme targeting the thrust roller bearing subjected to non-rotational oscillatory motion within the FPSO SYM system. Its core contribution lies in systematically addressing the challenge of fault feature extraction and identification for this distinctive bearing in strong-noise marine environments. By optimizing the key parameters of the Finite Impulse Response (FIR) filter in the Minimum Entropy Deconvolution method, this study enables MED to effectively enhance the weak fault impact components submerged in background noise, achieving the successful application of the MED method in the diagnosis of such oscillatory bearings. Building upon this, a joint diagnostic framework integrating 'MED filtering enhancement, quantitative assessment via time-domain indicators, and envelope spectrum analysis' is constructed, improving the salience of fault features. This research not only provides a reliable technical means for the safe operation and maintenance of soft yoke mooring leg bearings but also opens a new technical pathway for the condition monitoring of other widely existing non-rotational oscillatory components in marine engineering, demonstrating significant theoretical innovation and engineering application value.

2. Materials and Methods

2.1. Bearing Fault Diagnosis Methods

The SYM is one of the more commonly used mooring methods. For example, the Mingzhu FPSO, shown in Figure 1, utilizes the SYM. The SYM is suitable for shallow waters less than 50 m deep and generally consists of a mooring platform, yoke arm, mooring leg, ballast tank, and mooring bracket, as illustrated in Figure 2. The SYM connects the mooring platform and the vessel, maintaining the vessel's relative position. All components of the SYM are rigid parts, with universal joints between the mooring legs and yoke arms, as well as between the mooring legs and brackets, to ensure the FPSO vessel can perform normal rolling and pitching movements [15]. This prevents excessive loads from being exerted on the mooring platform. These universal joints consist of sliding bearings and thrust roller bearings. The thrust roller bearing at the upper hinge point of the mooring leg (shown as hinge X1 in Figure 2) is the core component of the SYM (as shown in Figure 3). It not only bears the enormous vertical load generated by the ballast tank but also allows the FPSO vessel structure to rotate around the mooring leg, minimizing the resultant force acting on the mooring platform. Therefore, if a fault occurs in this component, the FPSO cannot perform normal pitching, potentially leading to excessive force on the mooring platform,

which could cause structural damage or failure, severely impacting the stability and safety of the FPSO [16].



Figure 1. The Mingzhu FPSO.

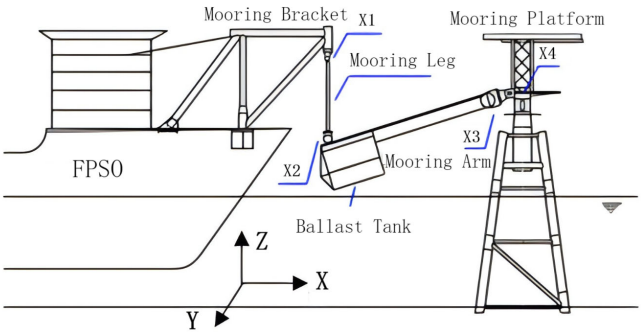

Figure 2. Soft yoke mooring system.

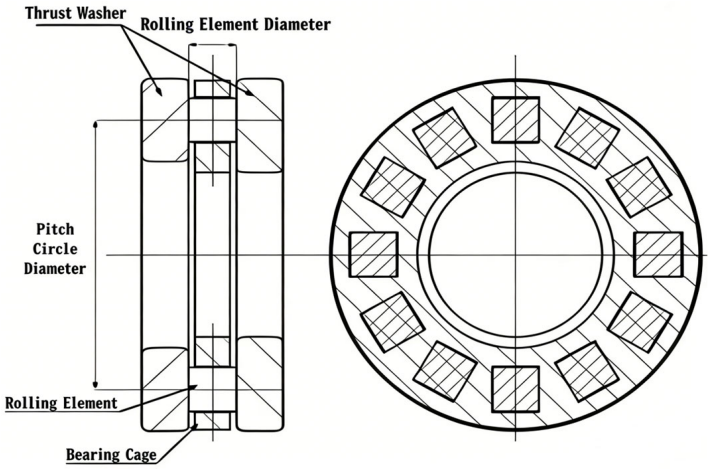

Figure 3. Thrust roller bearing.

This paper focuses on the damage diagnosis of thrust roller bearings in FPSO soft yoke mooring systems, with its research basis primarily derived from the special working conditions and critical role of such bearings in marine engineering. First, as the core load-bearing component of the articulated joint in the soft yoke, the thrust roller bearing operates long-term in a harsh marine environment characterized by high loads, strong corrosion, and variable conditions. Its motion pattern is non-rotational oscillatory swinging, which fundamentally differs from the working conditions of traditional rotating bearings. Under

this motion mode, the bearing is subjected to alternating stresses and impact loads, making it prone to damage such as fatigue pitting, wear, or even spalling on the raceways and rolling elements. Second, once damage occurs in the bearing, it directly affects the kinematic coordination of the soft yoke system. In mild cases, it causes abnormal vibrations and noise, accelerating structural fatigue; in severe cases, it may lead to the locking of local degrees of freedom, triggering load redistribution and stress concentration, thereby threatening the safety of the entire mooring system and even the FPSO itself. Therefore, conducting damage diagnosis research on such special bearings is not only a practical requirement for ensuring the reliable operation of the system but also an important subject for improving the theoretical framework of fault diagnosis for non-rotational moving components in marine engineering.

The methods for diagnosing rolling bearing faults are numerous. Among these, vibration-based bearing fault diagnosis methods are particularly effective at identifying and extracting features related to the fault impact characteristics of bearing structures. For example, time-frequency signal analysis methods like Short-Time Fourier Transform [17] and wavelet techniques [18,19] are widely used in monitoring and diagnosing various mechanical equipment due to their simplicity and efficiency. However, in a marine environment, the complex motion characteristics of FPSOs and the high-noise environment can cause fault signals to be submerged in noise signals. Therefore, it is necessary to filter and denoise the signal to highlight the fault pulse impact components within the signal before performing vibration signal analysis. The basic principle is as follows:

The original signal is received by the sensor through a certain path, a process known as convolution in engineering signal processing. Given the input signal $s(t)$ and the linear transmission system $H(t)$, the output signal $x(t)$ is the convolution of the two:

$$x(t) = H(t) * s(t) \tag{1}$$

If the output signal is known, solving for the input signal involves a process called deconvolution. When a fault occurs in the mooring leg thrust roller bearing of the FPSO, pulse impact signals $x(k)$ are generated at the fault site due to contact between the rolling elements and the raceways. After passing through a linear transmission system $h(n)$, the output $z(k)$ is

$$z(k) = h(n) * x(k) \tag{2}$$

where $z(k)$ is the signal received by the sensor.

The actual collected bearing vibration signal is often a convolution of the bearing fault pulse impact signal $x(t)$, large-scale random pulse signals $r(t)$, harmonic signals $d(t)$, and random noise signals $n(t)$ with the transmission path $h(m)$:

$$z(t) = (x(t) + r(t) + d(t) + n(t)) * h(m) \tag{3}$$

where $z(t)$ is the system's output signal received by the sensor. After isolating the bearing fault pulse impact signal from the system output signal, time-domain index analysis and envelope spectrum analysis methods can be used to extract relevant fault features.

Time-domain indices, as the simplest and most direct method, are widely used in diagnosing bearing vibration signals [20]. In this paper, the root mean square (RMS) value, crest factor, and kurtosis factor are used to evaluate the bearing condition [21], where:

Root mean square (RMS) value:

$$RMS = \sqrt{\frac{1}{N}\sum (x(t) - \overline{x})^2} \tag{4}$$

where N is the number of sampling points. For the vibration signal of a normal bearing, its mean value should be close to zero. The RMS value, also known as the effective value, represents the energy of the bearing signal and is an important indicator for judging the bearing's operating condition. When the bearing is fault-free, it operates smoothly without impact, and the RMS value is relatively small. As the bearing fault worsens, the RMS value increases accordingly [22].

Peak value:

$$peak = \frac{1}{2}(\max(x(t)) - \min(x(t))) \tag{5}$$

Peak value reflects the maximum amplitude of the bearing vibration signal; however, its application has inherent limitations. If the signal contains impact sequences caused by other factors not related to bearing faults, using the peak value as a diagnostic indicator can lead to distortion or even misjudgment.

Crest factor:

$$CrestFactor = \frac{peak}{RMS} \tag{6}$$

Crest factor is defined as the ratio of the signal's peak value to its RMS value. A higher ratio indicates more severe short-duration, high-amplitude vibrations within the acoustic signal.

Kurtosis factor:

$$kurtosis = \frac{1}{N}\sum\left(\frac{x(t) - \overline{x}}{\sigma}\right)^4 \tag{7}$$

where $\overline{x}$ is the arithmetic average of all observations in the dataset and σ is the sample standard deviation. The kurtosis factor reflects the degree to which the waveform deviates from a normal distribution. When the bearing is in the initial stage of a fault, the time-domain statistical indicators of the corresponding vibration signal increase. The kurtosis indicator reflects the degree of deviation from a normal distribution. When the bearing is operating normally, the vibration signal is approximately normally distributed, with a kurtosis value of about 3. A higher kurtosis value indicates a greater deviation from a normal distribution and is one of the most commonly used indicators in bearing diagnosis.

Envelope spectrum analysis is a frequency-domain analysis method that is insensitive to sinusoidal motion but sensitive to events related to impacts. This characteristic makes envelope demodulation analysis widely applicable in diagnosing mechanical equipment faults with impact characteristics. Currently, the main method for envelope analysis is using the Hilbert transform.

The Hilbert transform of a signal $s(t)$ is defined as follows:

$$h(t) = \frac{1}{\pi}\int_{-\infty}^{+\infty}\frac{s(\tau)}{t-\tau}d\tau = \frac{1}{\pi t} * s(t) \tag{8}$$

Let:

$$z(t) = s(t) + jh(t) \tag{9}$$

The envelope $E(t)$ of the signal $z(t)$ is defined as follows:

$$E(t) = |z(t)| = |s(t) + jh(t)| = \sqrt{s^2(t) + h^2(t)} \tag{10}$$

Envelope spectrum analysis focuses on short-duration impact signals, and its characteristics concerning the distribution of fault frequencies make it advantageous for bearing fault diagnosis [23,24]. However, since fault signals are submerged in noise, random pulses, and other harmonic components, directly performing envelope demodulation analysis on the signal is not very effective. Therefore, before envelope spectrum analysis, the signal must be processed to extract the fault impact signal from the original signal. Then, the

diagnosis is conducted using time-domain indices and envelope spectrum analysis by considering changes in the effective values of time-domain indices before and after the fault and comparing the peak frequencies in the envelope spectrum after the fault with the bearing fault characteristic frequencies.

This study did not directly employ general statistical methods for fault diagnosis, primarily for the following reasons. First, the bearing vibration signals collected in the marine environment are characterized by strong noise, non-stationarity, and multiple interferences. The assumptions underlying general statistical methods regarding signal distribution (such as normality and stationarity) are difficult to satisfy with such signals, limiting the effectiveness of feature extraction. Second, the "non-rotational oscillatory" motion mode of the thrust roller bearing results in non-fixed fault characteristic frequencies, making traditional statistical diagnostic models based on rotational frequency directly inapplicable. Furthermore, general statistical methods are often insensitive to transient impact components within the signal, whereas bearing damage precisely manifests as periodic or aperiodic impact events, necessitating more targeted signal enhancement and feature highlighting techniques. Therefore, this study adopts a strategy combining MED with time-domain indicators and envelope spectrum analysis. This approach aims to extract and enhance fault impact components from strong noise, thereby enabling effective identification of damage in non-stationary, non-rotational bearings. This method does not rely on prior statistical assumptions and is better suited to meet the practical diagnostic needs under complex marine working conditions.

2.2. Application of MED in Bearing Fault Diagnosis

This paper employs the MED method to isolate the bearing fault pulse impact signal from the output signal received by the sensor, which contains various noise signals and harmonic signals.

Since the entire process is one of entropy increase, the principle of minimum entropy deconvolution is to find an L-order inverse filter $g(l)$ that makes the output signal after passing through the inverse filter as deterministic as possible. This minimizes the amplitude spectrum entropy of the signal, thereby achieving the highest similarity between the obtained output signal and the original signal while retaining the main features of the original signal [25]. The relevant relationship is described as follows:

$$y(k) = \sum_{l=0}^{L-1} g(l) \cdot z(k-l) \approx \beta x(k-\tau) \tag{11}$$

where:

L	Order of the inverse filter;
k	Time index of the signal;
l	Coefficient index of the inverse filter;
β	Amplitude correction factor;
τ	Time delay correction factor.
$y(k)$	Output signal of the inverse filter at time k;
$z(k-l)$	The sampled value of the distorted observed signal;
$x(k-\tau)$	The original bearing fault impulse signal.

In the design of the inverse filter, blind deconvolution is required. The common methods mainly include the objective function method and the eigenvector method, with the objective function method being more widely used. Nandi and Lee et al. proposed using the m-th order cumulant as the objective function for deconvolution [26]:

$$o_m(g) = \frac{\sum_{i=1}^{N} y(i)^m}{\left[\sum_{i=1}^{N} y(i)^2\right]^{m/2}} \tag{12}$$

where:

N Total number of sampling points in the observed signal;

$o_m(g)$ Objective function based on the m-th order cumulant.

Generally, the cumulant order $m = 4$ is chosen, and considering that the entropy of the filtered signal should be minimized, the first derivative of the objective function is zero, that is,

$$\frac{\partial o_4(g)}{\partial g(l)} = 0 \tag{13}$$

From Equation (13), we can obtain the following: $\partial o_4(g)/\partial g(l) = 0$

$$\frac{\sum_{k=1}^{N} y(k)^2}{\sum_{k=1}^{N} y(k)^4} \cdot \sum_{k=1}^{N} y(k)^3 z(k-l) = \sum_{p=0}^{L-1} g(p) \cdot \sum_{k=1}^{N} z(k-l) z(k-p) \tag{14}$$

where:

p Coefficient index of the inverse filter.

Let:

$$b = \frac{\sum_{k=1}^{N} y(k)^2}{\sum_{k=1}^{N} y(k)^4} \cdot \sum_{k=1}^{N} y(k)^3 z(k-l) \tag{15}$$

$$A = \sum_{p=1}^{L-1} g(p) \tag{16}$$

$$g = \sum_{k=1}^{N} z(k-l) z(k-p) \tag{17}$$

Equation (15) can be rewritten as $b = A \cdot g$, where b is the cross-correlation vector between the input and output of the inverse filter, A is the Toeplitz autocorrelation matrix of the input signal of the inverse filter, and g is the parameter of the inverse filter. In this paper, an FIR filter is used as the inverse filter. The relevant parameters are the filter order, passband cutoff frequency, stopband cutoff frequency, attenuation rate, etc. The design steps are as follows: first, initialize the FIR filter parameters $g^{(0)}$, and calculate the corresponding output signal $y^{(0)}$ using the known signal and the FIR filter. Second, compute the filter parameter $g^{(t+1)}$ via the formula. Finally, use the following formula:

$$\begin{cases} E(err) = E\left[\frac{(g^{(t)} - \mu g^{(t-1)})}{\mu g^{(t-1)}}\right] \\ \mu = \left(\frac{E(g^{(t-1)})^2}{(E(g^{(t)})^2}\right)^{1/2} \end{cases} \tag{18}$$

where:

t Number of iterations;

μ Iteration weight adjustment factor.

Then, compare it with the convergence tolerance: when the error is greater than the convergence tolerance ($E(err) > tolerance$), repeat the previous steps until the error is smaller than the convergence tolerance to terminate the loop. At this point, the final filter parameter $g^{(end)}$ can be obtained; $y^{(end)}$ can then be calculated using this parameter, ultimately realizing the minimum entropy deconvolution algorithm.

This paper designs an FIR filter using the principle of minimum entropy deconvolution, selecting different filter orders, iteration counts, and termination conditions to examine the influence of filter parameters on the performance of the minimum entropy deconvolution

method. The final filter parameters are set as follows: the filter order is set to 30, the maximum number of iterations is set to 30, and the iteration termination condition is set to 0.01. The selection of the aforementioned FIR filter parameters is based on the following considerations: First, the filter order needs to be sufficiently long to capture the fault impact response, but an excessively long order may easily lead to overfitting. Pre-liminary tests have shown that when the order is around 30, the optimal balance between impact enhancement and waveform smoothness can be achieved. Second, the algorithm usually converges rapidly within 20 iterations, so setting the maximum number of iterations to 30 is sufficient to ensure convergence with a margin. The iteration termination condition is set to 0.01 based on empirical values, which can improve computational efficiency while ensuring convergence accuracy. This set of parameters is a stable operating point determined by comprehensively considering the effectiveness and computational efficiency of the algorithm, and its rationality has been supported by relevant research [27]. After filtering, random noise, harmonic signals, and large random pulse signal interference in the original signal are excluded. Considering the attenuation factors of the transmission path, the filter also highlights the pulse impact components in the signal. On this basis, mainly time-domain statistical parameters are used to compare the changes in time-domain indices before and after the fault, while envelope spectrum analysis is performed to consider frequency concentration phenomena or to find the characteristic frequency of the fault, comprehensively reflecting the type of fault in the bearing. The specific process is shown in Figure 4.

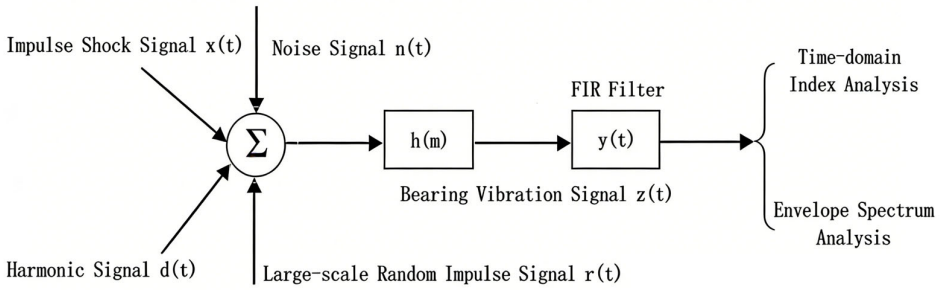

Figure 4. Flow chart of fault diagnosis.

2.3. Fault Signal Modeling of Rolling Bearings

For bearings where the shaft rotates periodically, their vibration signals exhibit cyclic and stationary characteristics. This paper mainly adopts the bearing signal model established by Macfadden to describe the pitting fault of FPSO mooring leg bearings. Since the impact period caused by the fault is extremely short, the motion period of the pitting position is longer than the impact period. During the operation of the bearing, a periodic impact train is generated. The pitting fault signal model of rolling bearings can be derived from the dynamic differential equations of rolling bearings [28,29]:

$$\begin{cases} ax(t) = \sum_{v=1}^{M} A_v s(t - vT - \tau_v) \\ A_v = A_0 \cos(2\pi Qt + \varphi_A) + C_A \\ s(t) = e^{-Bt} \cos(2\pi f_n t + \varphi_w) \end{cases} \quad (19)$$

where:

a Amplitude scaling factor;
M Number of fault impacts;
v Summation index;
A_v Amplitude value of the v-th fault impact;
T Fault impact interval;
τ_v Random time delay of the v-th impact;
A_0 Reference amplitude value of the impact;
Q Phase parameter related to bearing operation;
C_A Random constant;
B Damping coefficient;
f_n Natural vibration frequency of the system;
φ_A Initial phase of A_v;
φ_ω Initial phase of $s(t)$.

Equation (19) describes the amplitude of the v-th impact and the impact induced by the pitting fault.

Considering the complexity of the marine environment where the FPSO mooring system is located, such as the hull undergoing compound motions at other frequencies or the influence of other random loads on the system. To verify the stability of the MED method, large random pulses, harmonic components, and zero-mean stationary random noise are added. Among them, the large random pulse is defined as follows:

$$s_j(t) = e^{-B_j t} \cos(2\pi f_j t + \varphi_j) \tag{20}$$

where:
B_j Random pulse attenuation damping;
f_j Random pulse frequency;
φ_j Initial phase of $s_j(t)$.

The harmonic components are defined as follow:

$$h(t) = 0.5 \times (\cos(2\pi f_k t + \varphi_k) + 0.5 \times \cos(4\pi f_k t + \varphi_h)) \tag{21}$$

where:
f_k Fundamental frequency of the k-th harmonic component;
φ_k Initial phase of the fundamental frequency cosine term;
φ_h Initial phase of the second harmonic cosine term.

For the convenience of simulation analysis, f_k is defined as 13 Hz, φ_k as $\pi/6$, and φ_h as $-\pi/6$.

Finally, the pitting fault vibration signal model of the FPSO mooring leg thrust roller bearing is expressed as follows:

$$x(t) = ax(t) + 0.5 s_j(t) + h(t) + n(t) \tag{22}$$

where $n(t)$ is the zero-mean stationary random noise.

2.4. Simulation Signal Analysis of Raceway Faults

To verify the feasibility of the aforementioned method for bearing fault diagnosis, a vibration signal model for pitting faults of FPSO mooring leg bearings was first established. Subsequently, an FIR filter designed based on MED was utilized for signal filtering and denoising to highlight the impulse impact signals. Finally, combined with time-domain indicators and envelope spectrum analysis, the fault diagnosis capability of the MED method for the thrust roller bearings of FPSO mooring legs was comprehensively evaluated.

The simulated vibration signal for pitting faults of FPSO mooring leg bearings was constructed based on Equation (19). Among the parameters, the time-domain distribution law of the fault impulse signal was set in accordance with the yaw motion of the FPSO and the motion law of the mooring leg bearings. Since the bearing motion is not unidirectional rotation, the rotational frequency is uncertain, and thus the fault characteristic frequency cannot be predetermined. The other parameters are set as follows: sampling frequency $F_s = 10{,}000$ Hz, natural frequency of the system $F_n = 2000$ Hz, and attenuation coefficient $B_i = 400\ s^{-1}$.

To investigate the performance of the MED method, large random impulse signals with an attenuation coefficient $B_j = 800\ s^{-1}$ and a natural frequency $F_n = 7700$ Hz were superimposed on the aforementioned signal, aiming to verify the method's ability to resist random impacts. Additionally, a harmonic signal with a frequency $f_j = 13$ Hz and zero-mean stationary random noise were added, controlling the signal-to-noise ratio (SNR) to −18.98 dB. The composite signal and its respective components are illustrated in Figures 5 and 6.

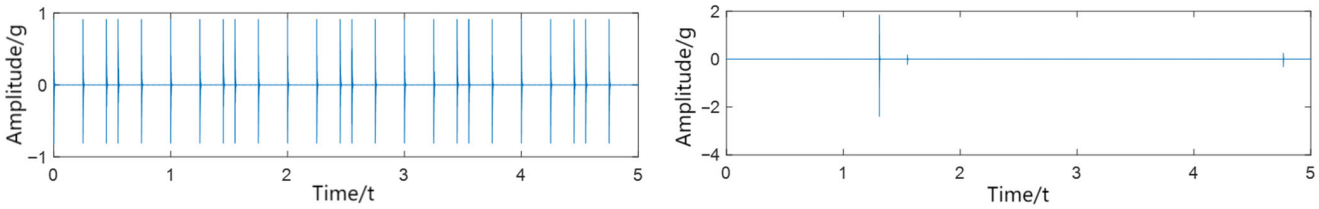

(**a**) Rolling track fault impact pulse signal (**b**) Large-scale random pulse impact pulse signal

Figure 5. Simulated pulse signal.

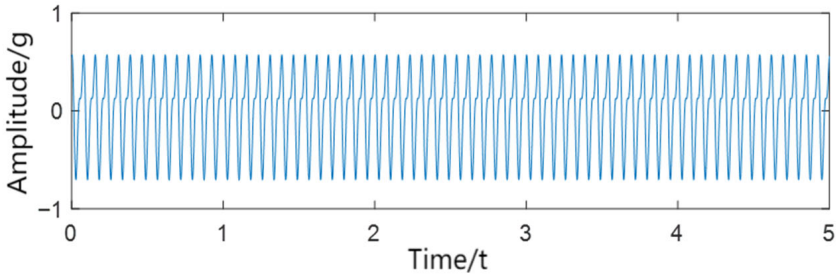

Figure 6. Harmonic component signal.

The parameters of the FIR filter are set as follows: the filter order is set to 30, the maximum number of iterations is set to 30, and the iteration termination condition is set to 0.01. Time-domain waveform diagram of the original signal with zero-mean stationary random noise added is shown in Figure 7, and its signal envelope is illustrated in Figure 8. It can be observed that the original signal waveform is submerged in noise and other interfering signals, with no obvious impulse impact waveform present. As can be seen from Figure 7, the impulse impact components of any fault signals cannot be directly identified from the envelope of the original signal. In the signal envelope spectrum shown in Figure 9, the phenomenon of frequency and energy concentration is not prominent; the peak frequencies include the harmonic signal frequency and some frequencies related to faults. However, the latter are not the main components in the envelope spectrum, making effective diagnosis impossible.

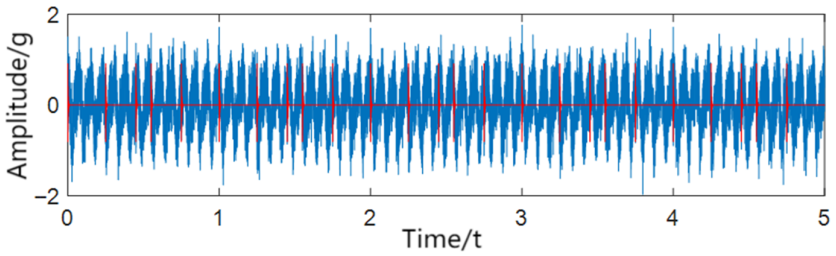

Figure 7. Time-domain waveform diagram of fault simulation signal before MED filtering (The red line is the rolling track fault impact pulse signal).

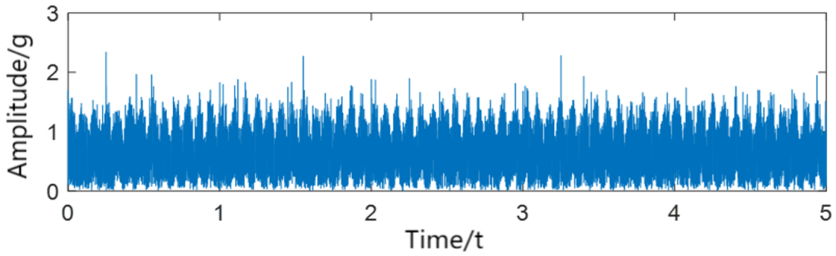

Figure 8. Time-domain envelope diagram of fault simulation signal before MED filtering.

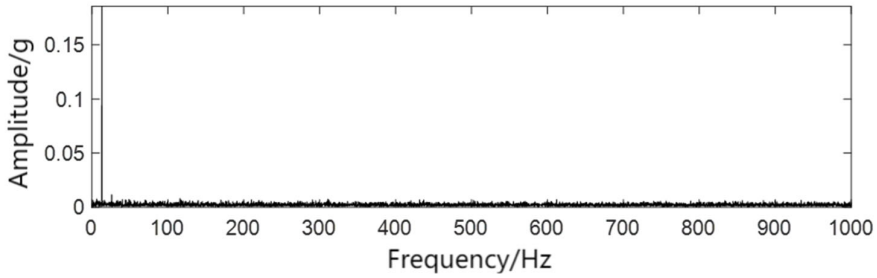

Figure 9. Envelope spectrum of simulated signal before MED filtering.

After denoising and filtering the original signal using the FIR filter designed based on the principle of Minimum Entropy Deconvolution, the time-domain waveform diagram is presented in Figure 10, and the signal envelope is shown in Figure 11. It can be seen that the fault impact components in both figures are enhanced and highlighted to varying degrees, and the impact components can even be directly observed from the envelope of the signal filtered by the FIR filter. In the signal envelope spectrum depicted in Figure 12, the signal frequency and energy are mainly concentrated below 500 Hz. Since the fault frequency is related to the impulse impact law, the impulse impact signal in this simulation is not set with significant periodicity, resulting in a "blurred" envelope spectrum of the signal. Nevertheless, some frequency components can still be obtained.

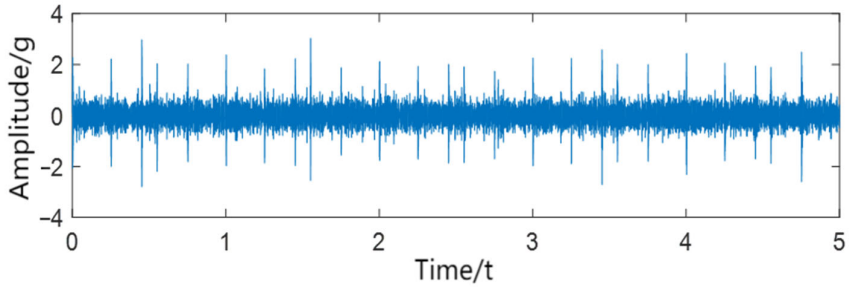

Figure 10. Time-domain waveform diagram of fault simulation signal processed by MED.

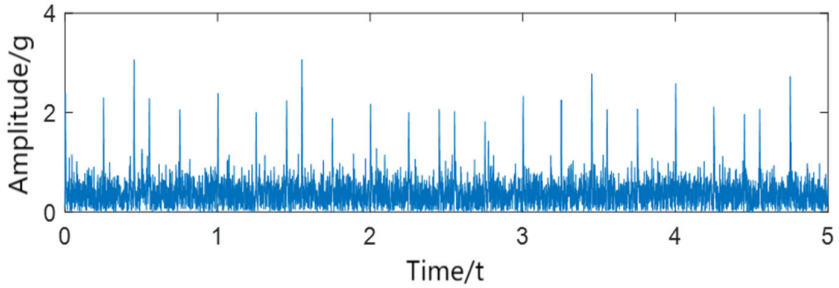

Figure 11. Time-domain envelope diagram of fault simulation signal processed by MED.

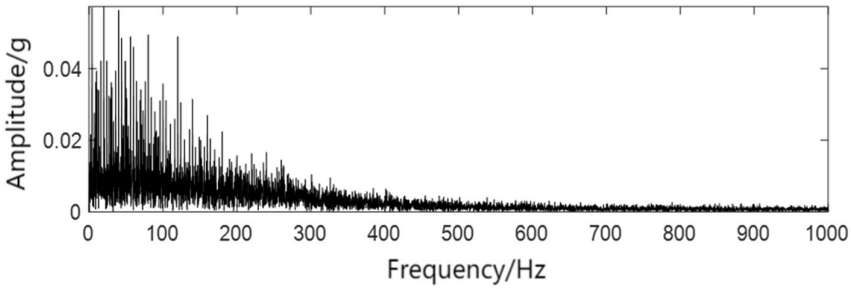

Figure 12. Envelope spectrum of fault simulation signal processed by MED.

To achieve comprehensive diagnosis, time-domain statistical indicators are integrated into the analysis, covering five key parameters: kurtosis, peak factor, root mean square value, impulse factor, and margin factor. A comparative analysis of these time-domain statistical indicators before and after filtering with the FIR filter designed based on the principle of Minimum Entropy Deconvolution is presented in Table 1.

Table 1. Comparison of time-domain statistical indicators before and after MED processing for simulated fault signals.

Time-Domain Statistical Indicators	Original Signal	Signal Processed by MED
Kurtosis	2.608	8.638
Peak factor	3.642	7.756
RMS value	0.500	0.354
Impulse factor	4.467	10.561
Margin factor	5.207	12.791

As shown in Table 1, among the five time-domain statistical indicators, the RMS value exhibits no significant variation, while other indicators such as kurtosis undergo substantial changes. In the process of bearing fault diagnosis, the greater the difference in time-domain statistical indicators of vibration signals between faulty and healthy bearings, the more conclusive it is that the bearing has developed a fault. Notably, after filtering with the FIR filter proposed in this study, the time-domain indicators of fault signals are effectively amplified, which facilitates the identification and diagnosis of bearing operating conditions.

2.5. Simulation Signal Analysis of Rolling Element Faults

To verify the diagnostic capability of the aforementioned method for bearing faults, this section mainly establishes a vibration signal model for rolling element faults of FPSO mooring leg bearings. Among them, the time-domain distribution law of the fault impulse signal is set in accordance with the yaw motion of the FPSO and the motion law of the mooring leg bearings. The time-domain indicators and envelope spectrum of the simulated normal vibration signal after denoising by the FIR filter designed based on the principle

of MED are investigated, with the aim of realizing a comparison with the simulated fault signal.

The simulated signal incorporates harmonic signals, large random impulse signals, and zero-mean stationary random noise signals in addition to the fault impulse impact signal, and the parameters of the FIR filter remain unchanged: the filter order is set to 30, the maximum number of iterations is set to 30, and the iteration termination condition is set to 0.01. Figure 13 illustrates the composition of the simulated signal.

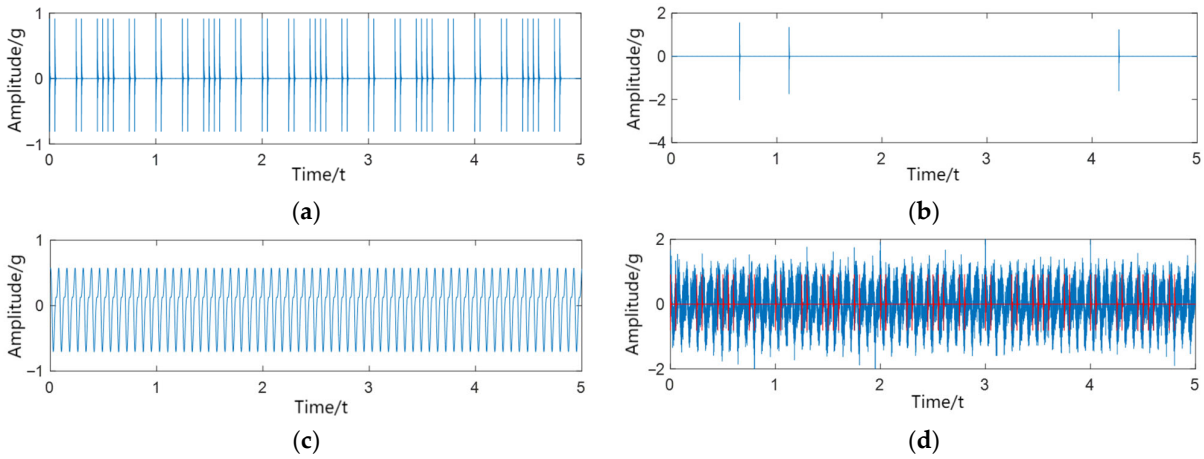

Figure 13. Composition of Rolling Element Fault Simulation Signal. (**a**) Rolling element fault impact pulse signal; (**b**) Large random pulse impulse signal; (**c**) Harmonic component signal; (**d**) Time-domain waveform with zero mean stationary random noise added (The red line is rolling element fault impact pulse signal).

Figures 13–15 show in sequence the time-domain waveform, time-domain envelope, and envelope spectrum of the rolling element fault signal after adding zero-mean stationary random noise. In the envelope spectrum shown in Figure 15, the harmonic signal frequency $f_j = 13$ Hz can be clearly observed as the peak frequency, which is consistent with the harmonic frequency of the fault signal. Figures 16–18 present the time-domain waveform, time-domain envelope, and envelope spectrum after denoising by the MED filter. Due to the uncertainty of the rotational frequency, there is no amplitude modulation of the fault impulse signal. In the envelope spectrum shown in Figure 18, the harmonic signal frequency $f_j = 13$ Hz exists, but the main components are related to the bearing fault characteristic frequencies, thereby verifying the reliability of the envelope detection method. As can be seen from Figure 18, the envelope spectrum after MED filtering exhibits a prominent spectral peak at 20 Hz, accompanied by equally spaced sideband components around it. The formation mechanism of this feature is directly related to the timing of the fault impacts set in the simulation model: within a single motion cycle, the fault pulses occur at 0.25 s, 0.5 s, 0.75 s, and 1.0 s, i.e., the impact interval is 0.25 s, corresponding to a fault-induced impact repetition frequency of 4 Hz. When this 4 Hz periodic impact acts on the bearing-support system, it excites a resonant response at the system's natural frequency. In this simulation, that resonant frequency is manifested as 20 Hz. Therefore, the structure observed in the envelope spectrum—centered at 20 Hz with 4 Hz sidebands distributed on both sides—accurately conforms to the fault characteristic pattern of "periodic impact—system resonance—amplitude modulation." Thus, 20 Hz can be clearly identified as the characteristic frequency of this rolling element fault. The simulation results clearly verify the identifiability of this diagnostic feature.

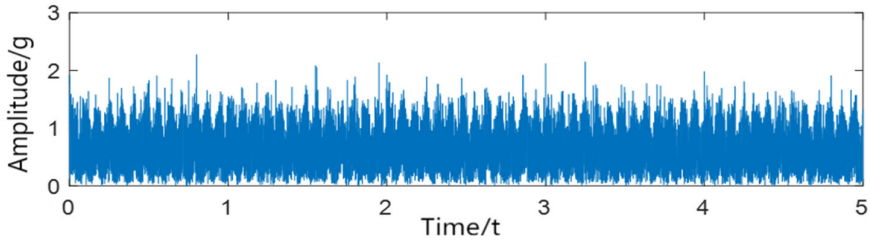

Figure 14. Time-domain envelope diagram of rolling element fault simulation signal.

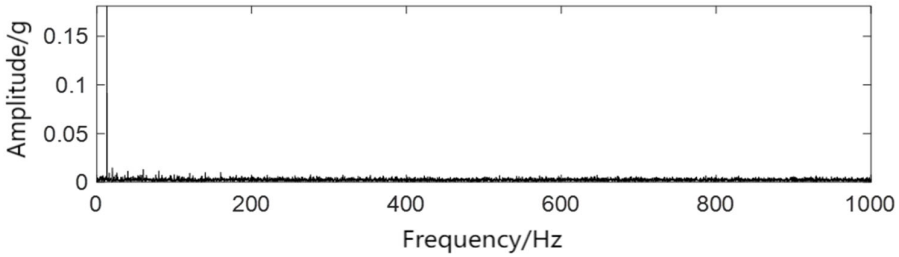

Figure 15. Envelope spectrum diagram of rolling element fault simulation signal.

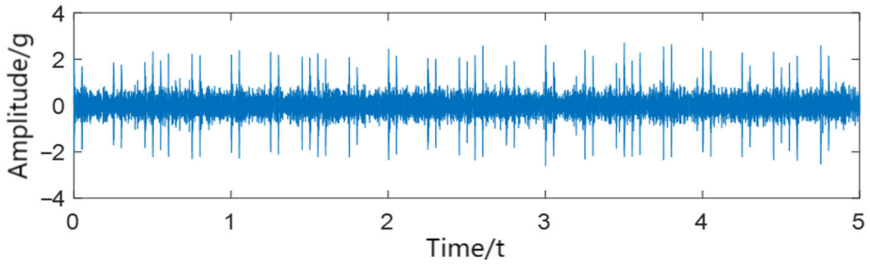

Figure 16. Time-domain waveform of rolling element fault simulation signal after MED filtering.

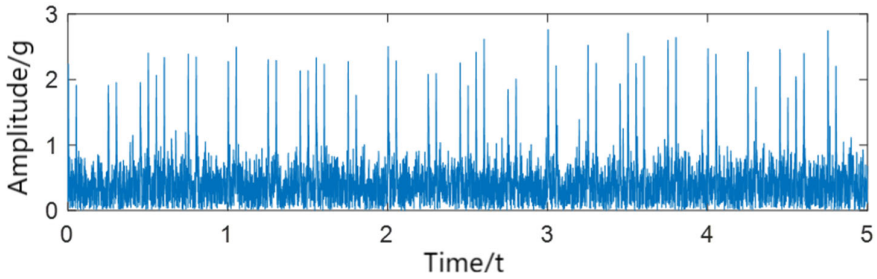

Figure 17. Time-domain envelope diagram of MED filtered simulation signal for rolling element faults.

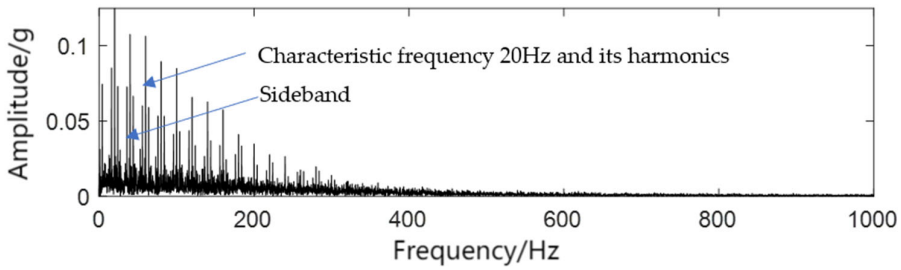

Figure 18. Envelope spectrogram of MED filtered simulation signal for rolling element faults.

The time-domain statistical indicators of the vibrational simulation signal for the bearing with rolling element fault are presented as follows.

As shown in Table 2, after processing with the MED filter, the corresponding time-domain statistical parameters have undergone significant changes, which indirectly reflects that these time-domain indicators possess a certain degree of stability in responding to fault characteristics. However, due to variations in the severity of bearing faults, the magnitudes of the time-domain indicators differ accordingly. Thus, time-domain statistical indicators can only be used to determine the severity of bearing faults, but not to identify the specific location of the faults. Table 2 also demonstrates the good stability of the FIR filter designed based on the principle of MED: its function is merely to highlight the impulse components in the signal, rather than excessively altering other characteristic parameters.

Table 2. Comparison of time-domain statistical indicators of vibration signals for bearings with rolling element faults before and after MED processing.

Time-Domain Statistical Indicators	Original Signal	Signal Processed by MED
Kurtosis	2.619	8.614
Peak factor	4.036	6.908
RMS value	0.504	0.397
Impulse factor	4.953	9.677
Margin factor	5.778	11.869

This section has completed the validity verification of the core diagnostic methods and key technologies. Specifically, this section has elaborated on two core diagnostic methods, namely time-domain statistical indicators and envelope spectrum analysis. On this basis, the feasibility of the proposed analysis and diagnostic methods has been systematically verified by constructing vibration signal simulation models for both normal and fault conditions. Simulation results confirm that the FIR filter designed based on the principle of MED exhibits excellent filtering, noise reduction, and deconvolution performance. Even under complex working conditions with strong noise interference and mixed large-scale random impact pulses, it can still effectively separate the original fault impact signals, providing reliable data support for subsequent fault feature extraction and diagnostic analysis.

2.6. Bearing Fault Experiment Method for Soft Yoke Mooring Legs

To verify the applicability of the aforementioned fault diagnosis method to the bearing fault diagnosis of soft yokes, this paper designed a model experiment conducted in the State Key Laboratory of Industrial Equipment Structure Analysis. In this experiment, a 1:10 scale model of the soft yoke mooring system was used, and a six-degree-of-freedom motion simulation platform was employed to simulate the vessel's motion conditions. The experimental system is shown in Figure 19.



Figure 19. Six-DOF motion simulation platform and FPSO mooring system.

Based on the analysis of the measured data from the FPSO soft yoke on-site, it is known that the pitch motion of the FPSO soft yoke has the greatest impact on the thrust roller bearings of the mooring system. Therefore, this paper focuses on simulating and experimenting with the pitch motion conditions. Considering that the amplitude and frequency of the actual FPSO pitch motion are not particularly large, the pitch amplitude in this experiment is controlled within 5°, and the pitch frequency is controlled within 0.35 Hz, and each set of the experiments are repeated three times. The designed experimental conditions are shown in Table 3. The bearing model used in the experiment is the NSK89307 thrust roller bearing (manufactured by Nippon Seiko Kabushiki-kaisha, Tokyo, Japan), which has the same structure as the thrust roller bearings used in the actual soft yoke. Electric spark machining was used to artificially create bearing pitting and wear faults, as shown in Figure 20. The main parameters of the experimental bearings are listed in Table 4.

Table 3. Test conditions.

Pitch Frequency	Pitch Amplitude					
0.1 Hz	±2	±3	±4	±5	±6	±7
0.2 Hz	±3	±3	±4	±5	±6	±7
0.3 Hz	±2	±3	±4	±5	\	\
0.35 Hz	±2	±3	±4	\	\	\



(**a**) (**b**)

Figure 20. Test bearing and its damage location. (**a**) Trouble of raceway of thrust roller bearing. (**b**) Trouble of roller of thrust roller bearing.

Table 4. Test objects and Structural parameters.

Bearing Model	NSK, 89307 Thrust Roller Bearing
Inner Ring Diameter	35.0 mm
Outer Ring Diameter	68.0 mm
Pitch Diameter	51.5 mm
Roller Radius	8 mm
Number of Rollers	12
Contact Angle β	90°

The arrangement of the sensors used in the experiment is shown in Figure 21. In this experiment, piezoelectric vibration acceleration sensors were used to measure fault signals, with a sensitivity of 99.8 mV/g. The sensors were rigidly fixed to the outer wall of the mooring leg at the bearing location using strong adhesive. Additionally, a video monitoring device was installed at the mooring leg bearing position to monitor the relative rotational condition of the bearings in real-time. The placement of the camera is shown in Figure 22.



Figure 21. The installation location of vibration acceleration.



Figure 22. The installation location of video surveillance.

3. Results

3.1. Analysis of Normal Bearing Vibration Signal

To better highlight the characteristics of bearing faults, the condition with a pitch frequency of 0.2 Hz and a pitch amplitude of $\pm 4^{\circ}$ was selected for processing and analysis. From the video monitoring, it can be observed that the upper hinge point of the mooring leg performs a pendulum-like motion, with its angular velocity constantly changing. When the bearing rotates to the other side's limit, there is a sudden stop action. To avoid the impact of this sudden stop on signal analysis, the signal processing in this paper is based on data from part of the motion cycle, specifically extracting 1.6 s from 2.5 s for signal processing.

Figure 23 shows the time-domain waveform of the undamaged bearing vibration signal and the time-domain waveform after filtering. In the time-domain signal after MED filtering, a pulse impact signal not caused by bearing faults is still mixed in, but other non-impact pulse parts become extremely smooth after MED filtering, which can confirm that the minimum entropy deconvolution method can highlight impact signals. Figure 24. shows the envelope spectrum of the normal signal, where peak frequencies appear at 0.2 Hz and 0.4 Hz, but they are not particularly prominent. Throughout the entire envelope spectrum, there is no frequency concentration phenomenon in the frequency domain, except for the primary pitch frequency of 0.2 Hz and its harmonic frequency of 0.4 Hz.

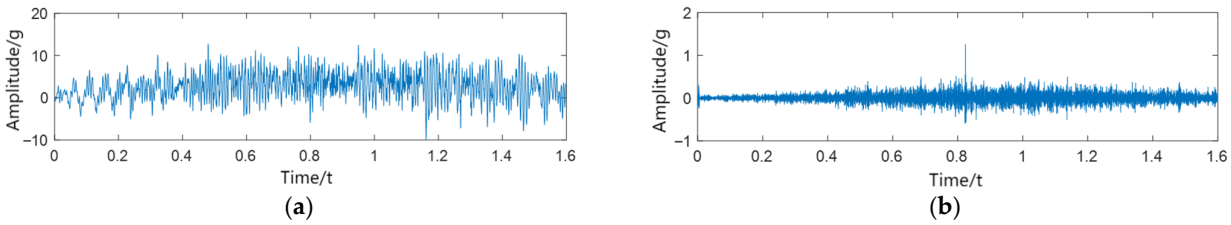

Figure 23. Time-Domain Waveform of Normal Bearing. (**a**) Time-domain waveform of the original signal; (**b**) Time-domain waveform of original signal filtered by MED.

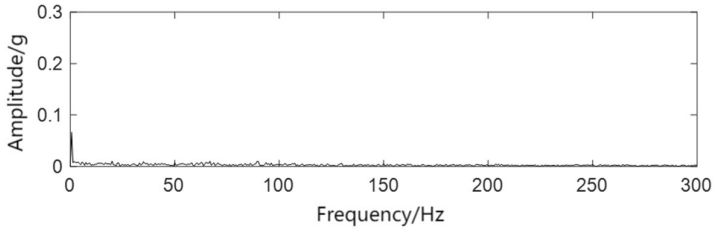

Figure 24. Spectrum envelope diagram of normal bearing.

3.2. Analysis of Vibration Signal During Bearing Raceway Fault

Figure 25 shows the time-domain waveforms of the same mooring leg under the same conditions as in Section 2.6, but with a bearing raceway fault. The figure includes the time-domain waveform of the signal with the fault and the time-domain waveform after MED filtering. It can be observed that after MED filtering, the fault impact pulses are prominently amplified (relative to Figure 23), while other types of vibrations show no significant changes. This verifies that the MED method can effectively isolate impact signals from harmonic and noise signals.

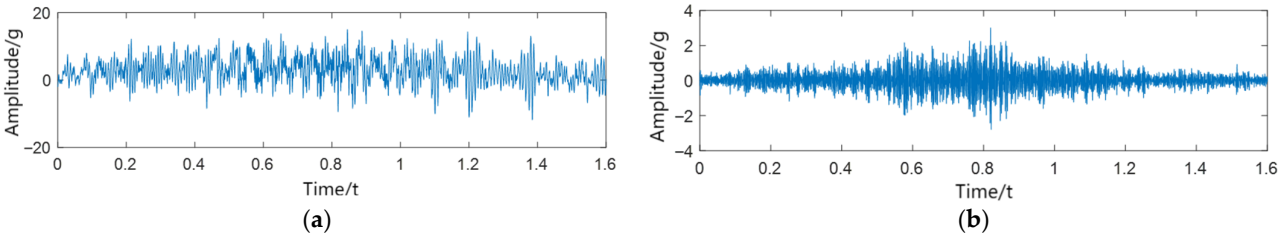

Figure 25. Time-domain signal waveform of bearing with raceway fault. (**a**) Time-domain waveform of the original signal; (**b**) Time-domain waveform of original signal filtered by MED.

Figure 26 presents the envelope spectrum of the vibration signal from the mooring leg's thrust roller bearing with a raceway fault, after MED filtering. Comparing this with Figure 24, both show a peak frequency at 0.2 Hz, which corresponds to the pitch frequency of the vessel. However, Figure 26 also reveals peaks at other frequencies. In mechanical equipment fault diagnosis, the occurrence of frequency concentration in the envelope spectrum indicates energy concentration, which suggests that the bearing's operating condition is abnormal. However, frequency concentration alone in the envelope spectrum does not fully explain the type or severity of the bearing fault.

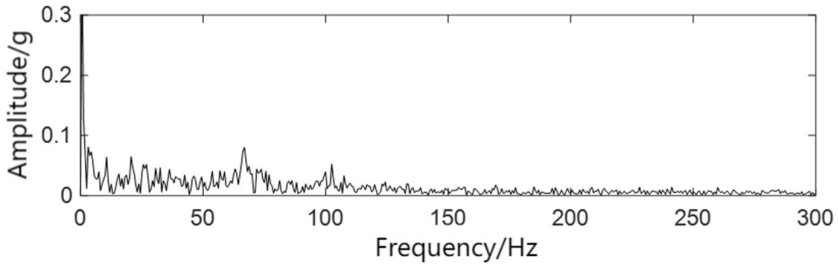

Figure 26. Envelope spectrum of bearing with raceway fault.

3.3. Analysis of Vibration Signal During Rolling Element Fault

For rolling element faults, considering the complexity of the rolling element's contact and motion, 10,000 data points with a duration of 2 s were extracted for analysis from the collected data. Figure 27 shows the time-domain waveform of the rolling element fault bearing at the extracted data points and the time-domain waveform after MED filtering. From Figure 27, it can be seen that after MED filtering, the fault impact pulse signals are

highlighted in the time-domain waveform. Figure 28 presents the envelope spectrum of the rolling element bearing signal, where peak frequencies at the motion frequency of 0.2 Hz and its harmonics are observed, along with many peaks at other frequencies. This indicates that the bearing's operating condition has become abnormal.

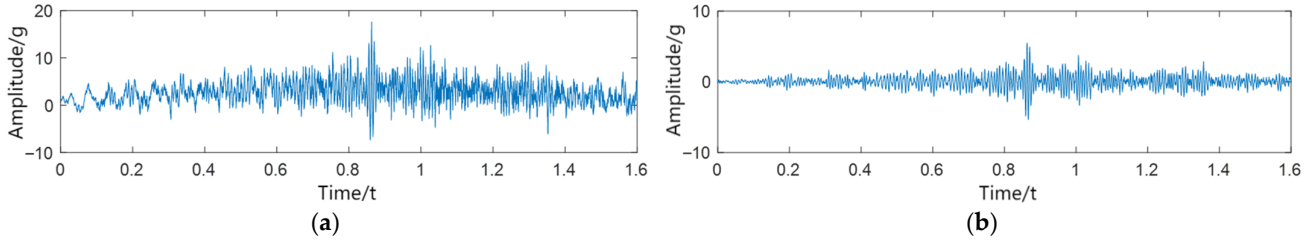

Figure 27. Time-domain waveform of rolling element fault bearing. (**a**) Time-domain waveform of the original signal; (**b**) Time-domain waveform of original signal filtered by MED.

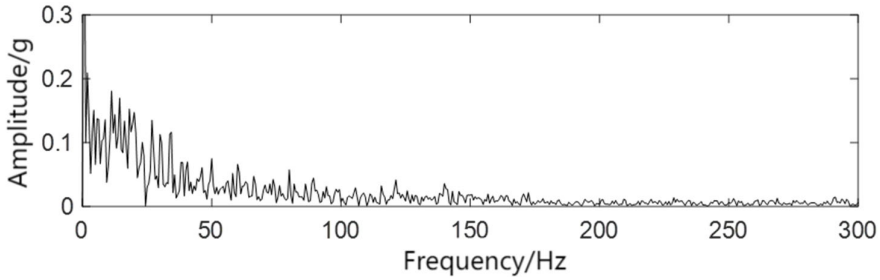

Figure 28. The envelope spectrum of rolling element fault bearing.

3.4. Analysis of Time-Domain Characteristic Indicators

The experimental results indicate that the MED method has a significant effect on enhancing the original pulse impact signals of faulty bearings. In bearing fault diagnosis, time-domain statistical indicators can clearly reflect the operating condition of the bearing. However, due to the complexity of the FPSO mooring system's motion and the uniqueness of its structure, the effectiveness of envelope spectrum analysis is not as prominent. Nonetheless, it can still reflect some characteristics of the fault, and can be used as an auxiliary tool for fault diagnosis.

Additionally, time-domain characteristic indicators for the normal state and two fault states of the FPSO mooring leg's thrust roller bearing are statistically summarized in Table 5.

Table 5. Comparative analysis of time-domain characteristic indicators.

	Normal Bearing	Raceway Fault	Rolling Element Fault
Kurtosis indicator	2.7536	3.1404	3.6738
Crest factor	2.8680	4.2637	4.9495
RMS value	3.2203	3.7594	2.3845
Impulse indicator	3.5379	5.3042	6.4179
Margin indicator	4.1343	6.2063	7.7184

From Table 5, it can be seen that various indicators show significant changes after a fault occurs. Among all the time-domain characteristic indicators, the kurtosis indicator demonstrates good sensitivity to rolling element and inner raceway faults and can be used as a primary criterion for these faults. For outer raceway and rolling element faults, the crest factor, impulse indicator, and margin indicator all show good sensitivity. The kurtosis indicator of a normal bearing vibration signal generally does not exceed 3. In this experiment, the kurtosis indicators for both the bearing raceway and rolling elements

exceeded 3, with rolling element faults showing a more pronounced increase. At the same time, the crest factor, impulse indicator, and margin indicator showed significant changes, indicating clear damage issues with the bearing. This suggests that the methods used in this study can effectively identify damage problems in bearings.

4. Discussion

The adaptive improvement scheme based on MED proposed in this study has successfully achieved accurate fault diagnosis of non-rotational thrust roller bearings at the hinge points of FPSO soft yoke mooring legs. Its core value lies in breaking through the adaptation bottleneck of traditional fault diagnosis methods under special swing conditions, and providing a new technical idea for the fault monitoring of non-rotational bearings in the marine engineering field.

From the perspective of the theoretical and practical significance of the research results, theoretically, this study is the first to adapt the MED method to the fault diagnosis scenario of non-rotational swing bearings. By optimizing the parameters of the FIR filter, it solves the problem of feature extraction of non-stationary signals, fills the research gap in the application of the MED method in special marine engineering conditions, and enriches the relevant content of "non-rotational moving part diagnosis" in the theoretical system of bearing fault diagnosis. Practically, the proposed method avoids the interference of traditional disassembly inspection on the normal operation of the FPSO mooring system, and overcomes the problem of low diagnostic accuracy of conventional vibration monitoring under strong noise and signal attenuation environments. It can directly provide technical support for the operation and maintenance of the FPSO soft yoke mooring system, and reduce downtime losses and safety risks caused by bearing faults.

Regarding the limitations of this study, an objective analysis should be carried out from the perspective of the differences between research conditions and practical application scenarios. First, the experiment only simulates a single pitching condition, and does not involve complex conditions such as rolling and wind–wave coupling. The main reason is that the preliminary experiment focuses on verifying the effectiveness of the core method, and it is necessary to first clarify the diagnostic performance under a single condition before gradually expanding to complex scenarios. However, in the actual marine environment, FPSOs often bear multiple motion loads simultaneously, which will make the nonlinear characteristics of bearing vibration signals more significant and may affect the universality of the method. In the future, the model needs to be improved through multi-condition joint experiments. Second, the diagnostic thresholds of time-domain indicators are determined based on small-sample experimental data, which is due to the high cost of artificially manufacturing faulty bearings (pitting, wear) and the limited sample size in the early stage. In practical applications, the fault severity has a continuous variation range, and the stability of small-sample thresholds is insufficient. It is necessary to further verify and revise them by expanding the sample size and covering mild, moderate and severe fault levels.

In summary, the adaptive improvement scheme based on MED proposed in this study provides an effective method for the fault diagnosis of non-rotational thrust roller bearings at the hinge points of FPSO soft yoke mooring legs, with clear theoretical innovation and practical value. Despite certain limitations, through the improvement and expansion of subsequent research, this method is expected to become one of the core technologies for fault monitoring of non-rotational bearings in the marine engineering field, providing more reliable guarantee for the safe operation of FPSOs and similar marine equipment.

5. Conclusions

This study focuses on the fault diagnosis challenge of non-rotational thrust roller bearings at the hinge points of FPSO soft yoke mooring legs, aiming to address the gaps in existing research, namely the lack of targeted diagnostic methods and the poor adaptability of mainstream techniques to swing conditions. To this end, an adaptive improvement scheme based on Minimum Entropy Deconvolution (MED) is proposed. By optimizing the parameters of the FIR filter (order L = 30, maximum number of iterations = 30, termination condition = 0.01), the scheme effectively adapts to the non-stationary characteristics of vibration signals under pendulum-like swing conditions. Combined with the joint analysis of time-domain indicators (kurtosis, peak factor, RMS value, etc.) and envelope spectrum, accurate fault diagnosis of raceway and rolling element faults is realized.

After three repeated experiments, the experimental results show that the proposed method significantly enhances the fault impact signals masked by strong noise and severe signal attenuation in the marine environment. After MED filtering, the kurtosis of fault signals increases from around 2.6 to more than 8.6, and the peak factor and pulse factor are also significantly amplified, making the fault characteristics more distinguishable. This scheme solves the problems of low efficiency and inaccuracy of traditional disassembly inspection and conventional monitoring methods, and fills the gap in the application of MED in the fault diagnosis of non-rotational bearings under swing conditions.

Compared with existing research, this study has significant advantages. Most existing studies on soft yoke mooring systems focus on overall structural safety early warning, with insufficient research on the diagnosis of core bearing components, which mostly rely on traditional methods combining displacement monitoring, strain monitoring and disassembly inspection, resulting in low efficiency and high misjudgment rate. In the field of general bearing fault diagnosis, although mainstream methods such as STFT and wavelet analysis are widely used, they are difficult to adapt to non-stationary signals and strong noise interference in the marine environment. The adaptive improvement scheme based on MED proposed in this study not only specifically solves the diagnosis problem of soft yoke mooring leg bearings through parameter optimization and joint analysis strategy, but also is superior to traditional methods in anti-interference ability and adaptability. Both simulation and experimental results show that even under strong noise with $SNR = -18.98$ dB and large-scale random impact pulse interference, the method can still effectively separate fault impact signals. This performance advantage makes it more suitable for complex marine conditions.

Nevertheless, this study has certain limitations. First, the experiments only simulate the single working condition of pitching motion, and do not consider the impact of complex marine working conditions such as rolling motion and wind–wave coupling, which may affect the universality of the method. Second, the diagnostic thresholds of time-domain indicators are determined based on small-sample experimental data, and their stability needs to be further verified by expanding the sample size and covering more fault severity levels.

For future research, the following directions are recommended to advance both the methodology and its practical application: First, a fault characteristic frequency correction model should be developed to resolve the envelope spectrum "blurring" caused by variable-speed swing conditions, potentially integrating order tracking or adaptive time-frequency analysis. Second, the experimental scope must be expanded to include complex multi-degree-of-freedom motions (e.g., combined pitching and rolling) and realistic environmental loads to validate and enhance the method's robustness. Third, research should focus on integrating this diagnostic scheme with real-time FPSO monitoring systems to enable online fault diagnosis and early warning capabilities. Finally, exploring the transferability of this adapted MED framework to other non-rotating or oscillatory components

in marine engineering would further demonstrate its broader value and establish a new benchmark for similar diagnostic challenges.

Author Contributions: Conceptualization and writing, Y.W.; methodology, J.Z.; formal analysis, S.S.; validation, Z.F.; funding acquisition, supervision and data curation, D.Z. funding acquisition and visualization, Y.H.; project administration and investigation, P.Z. project administration, supervision and resources, Z.J. All authors have read and agreed to the published version of the manuscript.

Funding: This work has been supported by the High-tech Ship Projects of the Ministry of Industry and Information Technology of China (Grant No. CBG2N21-4-1).

Data Availability Statement: Data is contained within the article.

Conflicts of Interest: The authors declare no conflicts of interest.

Abbreviations

The following abbreviations are used in this manuscript:

SYM	Soft Yoke Mooring
MED	Minimum Entropy Deconvolution
FIR	Finite Impulse Response
FPSO	Floating Production Storage and Offloading system
STFT	Short-Time Fourier Transform
SNR	signal-to-noise ratio

References

1. Wu, W.; Wang, Y.; Tang, D.; Yue, Q.; Du, Y.; Fan, Z.; Lin, Y.; Zhang, Y. Design, implementation and analysis of full coupled monitoring system of FPSO with soft yoke mooring system. *Ocean Eng.* **2016**, *113*, 255–263. [CrossRef]
2. Chen, B.; Sun, S.; Incecik, A.; Zhang, Z.; Ren, H. Nonlinear wave-structure-mooring interactions in hurricane condition: A case study using three-dimensional time-domain simulations. *Eng. Anal. Bound. Elem.* **2025**, *177*, 106233. [CrossRef]
3. Yang, X.; Cai, Y.; Song, A.; Li, J.; Yu, L. Development of monitoring and forecasting system for soft yoke moored FPSO. *Ship Eng.* **2014**, *36*, 198–201. [CrossRef]
4. Wang, Y.; Fan, Z.; Du, Y. Integrity assessment of soft yoke moored FPSO for the hinge point problems. In Proceedings of the Twenty-Fifth (2015) International Ocean and Polar Engineering Conference, Kona, HI, USA, 21–26 June 2015.
5. Zhang, Y.; Li, Y.; Kong, L.; Li, W.; Yi, Y. Rolling bearing condition monitoring method based on multi-feature information fusion. *J. Adv. Manuf. Sci. Technol.* **2023**, *3*, 2022020. [CrossRef]
6. Desnica, E.; Mikic, D.; Glavas, H.; Palinkas, I. Influence of diagnostics on bearing reliability on robotic systems. *Adv. Eng. Lett.* **2022**, *1*, 40–45. [CrossRef]
7. Pastukhov, A.; Timashov, E. Procedure for simulation of stable thermal conductivity of bearing assemblies. *Adv. Eng. Lett.* **2023**, *2*, 58–63. [CrossRef]
8. Pei, W.; Pei, X.; Xie, Z.; Wang, J. Research progress of marine anti-corrosion and wear-resistant coating. *Tribol. Int.* **2024**, *198*, 109864. [CrossRef]
9. Tang, J.; Lu, Y.; Bai, Z.; Gao, Q. Rolling bearing fault diagnosis based on synchronous compressed wavelet transform and CNN. *Sens. Microsyst.* **2022**, *41*, 130–133. [CrossRef]
10. Desnica, E.; Asonja, A.; Klajin, M.; Glavas, H.; Pastukhov, A. Analysis of bearing assemblies refit in agricultural PTO shafts. *Tech. Gaz.* **2023**, *30*, 872–881. [CrossRef]
11. Li, H.; Yu, Z.; Xiao, Y.; Li, Z.; Liu, H.; Li, B.; Shao, Q.; Gu, Z. Fault diagnosis of rolling bearings in gearboxes based on autocorrelation envelope and optimized MED. *Mech. Transm.* **2024**, *48*, 139–148. [CrossRef]
12. Qiao, Z.; Liu, Y.; Liao, Y. Application of improved empirical wavelet transform and minimum entropy deconvolution in railway bearing fault diagnosis. *J. Vib. Shock.* **2021**, *40*, 81–90. [CrossRef]
13. Fan, Z.; Sun, S.; Wang, Y.; Yue, Q.; Wang, Q. Design and research of soft yoke model experiment based on bearing fault diagnosis. *Exp. Sci. Technol.* **2021**, *19*, 1–6. [CrossRef]
14. Lyu, B.; Guo, C.; Wu, W.; Feng, J.; Yao, W.; Yue, Q. Hinge joint damage identification method of soft yoke mooring system based on multibody dynamic modeling and structural monitoring data. *Mar. Struct.* **2020**, *74*, 102808. [CrossRef]
15. Lyu, B.; Wu, W.; Yao, W.; Wang, Y.; Zhang, Y.; Tang, D.; Yue, Q. Multibody dynamical modeling of the FPSO soft yoke mooring system and prototype validation. *Appl. Ocean Res.* **2019**, *84*, 179–191. [CrossRef]

16. Liu, B.; Zhang, X. Failure analysis of YOKE in floating soft yoke mooring system. *Tianjin Sci. Technol.* **2014**, *41*, 47–50. [CrossRef]
17. Zhang, D.; Feng, Z. Application of iterative generalized short-time Fourier transform to fault diagnosis of planetary gearboxes. *Chin. J. Eng.* **2017**, *39*, 604–610. [CrossRef]
18. Zheng, J.; Pan, H.; Yang, S.; Cheng, J. Adaptive parameterless empirical wavelet transform based time-frequency analysis method and its application to rotor rubbing fault diagnosis. *Signal Process.* **2017**, *130*, 305–314. [CrossRef]
19. Liu, J.; Wang, W.; Golnaraghi, F.; Liu, K. Wavelet spectrum analysis for bearing fault diagnostics. *Meas. Sci. Technol.* **2008**, *19*, 015105. [CrossRef]
20. Guo, Q.; Wang, C.; Liu, P. Application of time-domain indicators and kurtosis analysis in rolling bearing fault diagnosis. *Mech. Transm.* **2016**, *40*, 172–175. [CrossRef]
21. Zhan, L.; Ma, F.; Zhang, J.; Li, C.; Li, Z.; Wang, T. Fault feature extraction and diagnosis of rolling bearings based on enhanced complementary empirical mode decomposition with adaptive noise and statistical time-domain features. *Sensors* **2019**, *19*, 4047. [CrossRef]
22. Song, L.; Wang, H.; Chen, P. Vibration-based intelligent fault diagnosis for roller bearings in low-speed rotating machinery. *IEEE Trans. Instrum. Meas.* **2018**, *67*, 1887–1899. [CrossRef]
23. Nikolou, N.G.; Antoniadis, I.A. Rolling element bearing fault diagnosis using wavelet packets. *NDT E Int.* **2002**, *35*, 197–205. [CrossRef]
24. Hu, Y.; An, G.; Wang, K.; Wang, C. Research on fault identification of rolling bearings based on wavelet adaptive envelope demodulation technology. *Coal Mine Mach.* **2010**, *31*, 214–217. [CrossRef]
25. Wang, Y.; Hu, N.; Hu, L.; Cheng, Z. Rolling Bearing Fault Diagnosis Based on Multipoint Optimal Minimum Entropy Deconvolution Adjusted Technique and Direct Spectral Analysis. In Proceedings of the Prognostics and System Health Management Conference (PHM), Harbin, China, 9–12 July 2017; IEEE: Piscataway, NJ, USA, 2017. [CrossRef]
26. Lee, J.-Y.; Nandi, A.K. Extraction of impacting signals using blind deconvolution. *J. Sound Vib.* **2000**, *232*, 945–962. [CrossRef]
27. Sawalhi, N.; Randall, R.B.; Endo, H. The enhancement of fault detection and diagnosis in rolling element bearings using minimum entropy deconvolution combined with spectral kurtosis. *Mech. Syst. Signal Process.* **2007**, *21*, 2616–2633. [CrossRef]
28. McFadden, P.D.; Smith, J.D. The vibration produced by multiple point defects in a rolling element bearing. *J. Sound Vib.* **1985**, *98*, 263–273. [CrossRef]
29. Ruan, D.; Chen, Y.; Gühmann, C.; Yan, J.; Li, Z. Dynamics modeling of bearing with defect in Modelica and application in direct transfer learning from simulation to test bench for bearing fault diagnosis. *Electronics* **2022**, *11*, 622. [CrossRef]

Disclaimer/Publisher's Note: The statements, opinions and data contained in all publications are solely those of the individual author(s) and contributor(s) and not of MDPI and/or the editor(s). MDPI and/or the editor(s) disclaim responsibility for any injury to people or property resulting from any ideas, methods, instructions or products referred to in the content.